SARS-CoV-2 infects and damages the mature and immature olfactory sensory neurons of hamsters

Anna Jinxia Zhang[1,2,3,*], Andrew Chak-Yiu Lee[2,*], Hin Chu[1,2,3,*], Jasper Fuk-Woo Chan[1,2,3,4,*], Zhimeng Fan[2], Can Li[2], Feifei Liu[2], Yanxia Chen[2], Shuofeng Yuan[1,2,3], Vincent Kwok-Man Poon[2], Chris Chung-Sing Chan[2], Jian-Piao Cai[2], Kenneth Lap-Kei Wu[5,6], Siddharth Sridhar[1,2,3,4], Ying-Shing Chan[5,6], Kwok-Yung Yuen[1,2,3,4,#]

[1]State Key Laboratory of Emerging Infectious Diseases, The University of Hong Kong, Pokfulam, Hong Kong Special Administrative Region, China.

[2]Department of Microbiology, Li Ka Shing Faculty of Medicine, The University of Hong Kong, Pokfulam, Hong Kong Special Administrative Region, China.

[3]Carol Yu Centre for Infection, The University of Hong Kong, Pokfulam, Hong Kong Special Administrative Region, China.

[4]Department of Microbiology, Queen Mary Hospital, Pokfulam, Hong Kong Special Administrative Region, China.

[5]School of Biomedical Sciences, Li Ka Shing Faculty of Medicine, The University of Hong Kong, Hong Kong Special Administrative Region, China.

[6]State Key Laboratory of Brain and Cognitive Sciences, The University of Hong Kong, Pokfulam, Hong Kong Special Administrative Region, China.

*These authors contributed equally

#**Corresponding author:**

Kwok-Yung Yuen

Email: kyyuen@hku.hk

Summary: Besides acute inflammation at OE, infection of mature and immature olfactory neurons, and the supporting sustentacular cells by SARS-CoV-2 may contribute to the unique olfactory dysfunction of COVID-19 which is not reported with SARS-CoV.

ABSTRACT

Background: Coronavirus Disease 2019 (COVID-19) is primarily an acute respiratory tract infection. Distinctively, a substantial proportion of COVID-19 patients develop olfactory dysfunction of uncertain underlying mechanism which can be severe and prolonged. The roles of inflammatory obstruction of the olfactory clefts leading to conductive impairment, inflammatory cytokines affecting olfactory neuronal function, destruction of olfactory neurons or their supporting cells, and direct invasion of olfactory bulbs, in causing olfactory dysfunction are uncertain.

Methods: In this study, we investigated the location for the pathogenesis of SARS-CoV-2 from the olfactory epithelium (OE) of the nasopharynx to the olfactory bulb of golden Syrian hamsters.

Results: After intranasal inoculation with SARS-CoV-2, inflammatory cell infiltration and proinflammatory cytokine/chemokine responses were detected in the nasal turbinate tissues which peaked between 2 to 4 days post-infection with the highest viral load detected at day 2 post-infection. Besides the nasopharyngeal pseudo-columnar ciliated respiratory epithelial cells, SARS-CoV-2 viral antigens were also detected in the more superficial mature olfactory sensory neurons labeled by olfactory marker protein (OMP), the less mature olfactory neurons labelled by Tuj1 at more basal position, and the sustentacular cells which provide metabolic and physical support for the olfactory neurons, resulting in apoptosis and severe destruction of the OE. During the whole course of infection, SARS-CoV-2 viral antigens were not detected in the olfactory bulb.

Conclusions: Besides acute inflammation at OE, infection of mature and immature olfactory neurons, and the supporting sustentacular cells by SARS-CoV-2 may contribute to the unique olfactory dysfunction of COVID-19 which is not reported with SARS-CoV.

INTRODUCTION

Severe acute respiratory syndrome coronavirus 2 (SARS-CoV-2) is a novel betacoronavirus that causes Coronavirus Disease 2019 (COVID-19) which was first identified in Wuhan, China in late 2019 [1-3]. Due to its high transmissibility and rapid global spread, the World Health Organization (WHO) declared the COVID-19 outbreak a pandemic [4]. COVID-19 has affected over 11 million patients with more than 0.5 million deaths globally within 6 months [2, 5]. Besides fever, upper and lower respiratory symptoms [6], olfactory dysfunction as manifested by partial or complete loss of olfactory function (hyposmia/anosmia), and dysgeusia have been frequently reported [7-11]. In our recent case control study cohort, olfactory symptoms were reported by 12 of 18 (67%) COVID-19 patients, often without (83%) concomitant rhinorrhea or nasal congestion at a median of 0.5 days after symptom onset. Most recovered within 14 days from onset of olfactory symptoms but some had refractory and disabling anosmia [12].

Odors are sensed by chemosensory organs located within the mammalian nasal cavity. The odor sensory signals are sensed by odorant receptors on olfactory sensory neurons (OSNs) and conducted to olfactory bulbs of the brain. Respiratory viruses can cause olfactory dysfunction by inflammatory obstruction of olfactory clefts, damage to OSNs and/or olfactory bulbs, and cytokine dysregulation in nasal turbinates [13-15]. However, few COVID-19 patients with olfactory dysfunction had prominent nasopharyngitis, rhinosinusitis, or obliteration of olfactory cleft on computerized tomographic imaging. This atypical feature raises the possibility of direct OSNs infection-induced damage by SARS-CoV-2. Currently, evidence of olfactory dysfunction predominantly based on clinical history, questionnaires and occasionally smell identification tests [7-9, 11]. Experimental evidence showing direct

association between SARS-CoV-2 infection and olfactory dysfunction is scanty. We recently demonstrated that SARS-CoV-2 could infect cells of neuronal origin *in vitro* [16]. Moreover, SARS-CoV-2 antigen could be readily detected in the nasal turbinate tissue in our recently established hamster infection model [2]. Inflammation-associated transient olfactory dysfunction has been implicated in human coronavirus 229E infection [15] but direct coronavirus infection of the human OSN has not been documented. Here, we investigated SARS-CoV-2 infection of hamster olfactory tissues and demonstrated the pathological consequence at the OE resulting from SARS-CoV-2 infection. Overall, our study provided evidence of direct SARS-CoV-2 infection of OSN, which contributed to our understanding on the olfactory dysfunction in COVID-19 patients.

METHODS

Virus and animals

SARS-CoV-2 virus HKU-001a strain (GenBank accession number: MT230904) was cultured and titrated in VeroE6 cells as previously reported and stored at −80°C until use [16]. Animal infection experiments were performed as we described previously with slight modifications [17]. Male and female golden Syrian hamsters, aged 6-8 weeks old, were obtained from Chinese University of Hong Kong Laboratory Animal Service Centre through the Laboratory Animal Unit of the University of Hong Kong (HKU). The animals were kept in Biosafety Level-2 (BSL-2) facility with free access to standard pellet feed and water. A challenge dose of 1×10^5 plaque forming units (PFU) of SARS-CoV-2 in 100µl of Dulbecco's Modified Eagle's Medium (DMEM) was intranasally inoculated to each hamster through under

intraperitoneal ketamine (200mg/kg) and xylazine (10mg/kg) anesthesia. Three hamsters were sacrificed for virological and histological analyses at each of the following time points: 12 hours post-inoculation (hpi), 2 days post-inoculation (dpi), 4dpi, 7dpi, and 14dpi. Three mock-infected control hamsters were included in the study for comparison. All experiments involving live SARS-CoV-2 were performed in the HKU BSL-3 facility following the approved standard operating procedures. Approval was obtained from the HKU Committee on the Use of Live Animals in Teaching and Research for the animal experiments (CULATR #5370-20).

Histological assessment and immunofluorescence staining of hamster nasal turbinate and brain tissues

These were performed as we previously described [17]. Briefly, 10% formalin-fixed hamster nasal turbinate and brain tissues were stained by hematoxylin and eosin (H&E), and immunofluorescence-stained for viral N protein (NP), olfactory marker protein (OMP), and neuron-specific class III β-tubulin (Tuj1). Staining for ACE2 expression was performed by immunohistochemistry. To identify apoptosis, Click-iT® Plus terminal deoxynucleotidyl transferase (TdT) dUTP nick-end labelling (TUNEL) (ThermoFisher, MA, USA) was used according to the manufacturer's instructions. All tissue sections were examined and the images were captured with Olympus BX53 semi-motorized fluorescence microscope using cellSens imaging software. Detailed methods were included in Supplementary Materials.

Determination of viral load in nasal turbinate tissues

Viral RNA load and infectious virus titer in hamster nasal turbinate tissues were determined by qRT-PCR and $TCID_{50}$ assays as we previously described [17, 18].

Cytokine and chemokine profiling

The relative expression levels of key cytokine/chemokine genes in homogenized nasal turbinate tissues were determined by qRT-PCR with the house-keeping gene β-actin used as control to normalize the amount of RNA as we described previously with slight modifications [17] (See Supplementary Table 1).

Statistical analysis

One-way ANOVA was used for analysis and comparison viral load and cytokine expression levels between different time points. A value of $P < 0.05$ was considered statistically significant.

RESULTS

SARS-CoV-2 readily infected olfactory epithelium of Syrian hamster

Using 6-8weeks old male or female hamster, we first demonstrated the composition of olfactory tissue, which composed of multiple layers of OSNs, sandwiched by sustentacular cells (SCs), and basal cells (BCs) (Figure 1A). Mature olfactory sensory neurons (mOSN) express olfactory marker protein (OMP), which can be utilized as a cell type marker [19]. By immunofluorescence staining, we revealed the distribution pattern of mOSN in hamster, which situated in the middle layer of OE with cytoplasmic expression of OMP (Figure 1B, solid arrowheads and Supplementary Figure 1A). Neuron-specific class III β-tubulin (Tuj1) is another commonly used neuron marker which has been used to identify immature neurons (iOSN) that are newly generated from olfactory stem cells [20]. In hamster OE, Tuj1 protein was shown in the dendrites, axons, and cell bodies of iOSNs (Figure 1B, open arrowheads and Supplementary Figure 1B). Deep to OE is the lamina propria (LP), which contains Bowman's glands, nerve fibers, and blood vessels. These findings were consistent with previously reported OE structures in mammalian species including rodents and humans [21-23].

To investigate SARS-CoV-2 infection in olfactory tissue, 10^5 PFU of SARS-CoV-2 was intranasally inoculated to hamsters and nasal turbinate tissues were collected at 12 hours, 2, 4, 7, 14 days post-infection (hpi, dpi). Viral RdRp gene was detected in homogenized tissues and was found to peak at 4dpi (Figure 1C, left panel), while the infectious viral titer ($TCID_{50}$) peaked earlier at 2dpi and became undetectable at 7dpi (Figure 1C, right panel). At 12hpi, the olfactory epithelium and respiratory epithelium were largely intact with some submucosal infiltration (Figure 1D, upper panels, black arrows). SARS-CoV-2 N protein (NP)

scattered in the epithelium (white arrowheads), and associated with cell debris (white arrows). This indicated epithelial cell damage upon SARS-CoV-2 infection already occurred at 12hpi. At 2 and 4dpi, both tissue destruction and the NP expression increased with time. OE showed increased intra-epithelial and submucosal infiltration, severe epithelial desquamation and accumulation of luminal cell debris (Figure 1D, black arrows). NP was extensively expressed and widely distributed in the OE and detached cell debris (Figure 1D, white arrowheads and arrows). At 7dpi, the epithelium of OE appeared intact, but cell debris mixed with secretion in the nasal cavity could still be detected, which occasionally contained NP positive cells (Figure 1D, bottom, arrows). These data indicated nasal mucosal epithelium and olfactory epithelium are highly susceptible to SARS-CoV-2 infection.

SARS-CoV-2 directly infected olfactory neurons

We next asked whether SARS-CoV-2 could directly infect olfactory neurons. Based on cell morphology, our result suggested that in addition to the respiratory epithelial cells (Figure 2A), SARS-CoV-2 NP expression were found in various cell type of OE that resembled the SCs, OSNs, BCs and Bowman's glands (Figure 2B), suggesting a broad cell tropism of SARS-CoV-2 at OE. Using double immunofluorescence studies, we further demonstrated the abundant presence of SARS-CoV-2 NP expression within the OMP-expressing neurons layer in the OE and localized in OMP expressing cells (Figure 2C arrowhead). Since all the cell types in OE are arranged tightly, we examined closely the SARS-CoV-2 infection caused desquamated neurons, we identified NP expression in detached OMP expressing cells clearly and excluded the interference from the staining signals of overlapping cells (Figure 2D arrowheads and Supplementary Figure 2A & 2B). Our results indicated that mOSN [24]

were infected by SARS-CoV-2. In addition, we also demonstrated NP expression in Tuj1-expressing iOSNs (Figure 2E, arrowheads). The intensity of NP expression indicated that most of the SARS-CoV-2 infected cells in hamster OE were non-neuronal cells (Figure 2). The sustentacular cells in the apical region of the OE were extensively infected as readily distinguished by morphology (Figure 2E, arrows). Further, angiotensin-converting enzyme 2 (ACE2) were detected by immunohistochemistry staining in hamster OE, mostly on the apical surface of respiratory and olfactory epithelium and submucosal glands; while scatter ACE2 expressing cells were also observed in the middle layer of olfactory epithelium which resemble olfactory neurons (Supplementary Figure 3). This ACE2 expression pattern was similar to previously reported by others [25, 26], and suggesting ACE2 could serve as the entry receptor for SARS-CoV-2 infection of olfactory cells.

SARS-CoV-2 infection induced proinflammatory cytokine/chemokine responses and tissue destruction in the nasal turbinate tissue

Direct infection and virus-induced inflammatory responses could both lead to tissue damage. Significant induction of proinflammatory cytokine and chemokine gene expression was detected upon SARS-CoV-2 infection. Specifically, IL-1β, IL-6, TNF-α MIP1-α, RANTES and IP-10 peaked at 2dpi to 4dpi and reduced at 7dpi (Figure 3A). In contrast, the IFN-α and IFN-γ were not significantly activated comparing to mock-infected hamsters (Figure 3A). Histologically, the most severe pathological damages in OE were observed at 4dpi, which showed massive immune cell infiltration and luminal secretion in the nasal cavity (Figure 3B, arrows). In addition, epithelial cells detachment and OE desquamation of a large regional apical layer were also observed (Figure 3B, arrowheads). Importantly, substantial terminal

deoxynucleotidyl transferase dUTP nick end labeling (TUNEL) staining along the disrupted OE was identified, which suggested SARS-CoV-2 infection triggered OE apoptosis (Figure 3C, left panels). Moreover, TUNEL signals were found to co-localize with both detached and intact OMP-positive mOSNs (Figure 3C, middle panel, white arrows), which was not observed in the OE of mock-infected hamsters (Figure 3C, right panel).

Although current clinical data suggested that olfactory dysfunction in COVID-19 patients are generally transient [27], the expression of viral antigen in the basal layer of hamster OE suggested that the neuron progenitor cells could be infected (Figure 2B, BC), which might cause a more long lasting olfactory impairment. In this regard, we showed that the morphology of OE was intact at 7dpi and 14dpi (Figure 4A and B, left panels). The cell proliferation marker, Ki67, was detected at day 7 dpi in apical layer of sustentacular cells and basal layer of OE (Figure 4A). At 14dpi, the number of Ki67 expressing cells was reduced in the apical layer, while still highly expressed in basal layer (Figure 4B), indicating regeneration of olfactory tissues occurred after SARS-CoV-2 infection.

SARS-CoV-2 might spread from the nasal cavity to olfactory bulbs of the brain through antegrade axonal spread. Examination of the brain at 2 and 4dpi showed no viral NP expression and no apparent histopathological changes in the olfactory bulbs (Supplementary Figure 4A) and in other part of the brain. However, a few TUNEL positive cells were found in glomerular layer (GL) area of the olfactory bulb of SARS-CoV-2-infected but not mock-infected hamster (Supplementary Figure 4B).

DISCUSSION

Acute infections by upper respiratory viruses such as influenza virus, parainfluenza virus, and rhinovirus are often associated with loss of smell. In most cases, it is due to conductive or obstructive change of the nasal cavity secondary to nasal mucosal edema [14, 15]. Occasionally, the virus directly infects and damages the olfactory sensory neurons or even olfactory bulb leading to persistent olfactory dysfunction [28]. In the current COVID-19 pandemic, a large proportion of SARS-CoV-2-infected patients reported symptoms of olfactory dysfunction with uncertain mechanisms [7-11]. We recently demonstrated that the OE at the nasal turbinate of SARS-CoV-2-infected hamsters was NP positive, suggesting direct SARS-CoV-2 infection of OE [2]. Sia and colleagues further showed that NP and Tuj1 could be visualized in close proximity in OE tissues of infected hamsters [29] and Bryche et al. demonstrated that transient damage of the OE is associated with the infection of sustentacular cells but not OSNs [30]. Here, by utilizing the hamster infection model, we demonstrated SARS-CoV-2 NP expression in Tuj1-expressing iOSN. Moreover, using olfactory marker protein (OMP) [19], we showed that mOSNs were infected by SARS-CoV-2. Importantly, severe destruction and detachment of mOSNs occurred upon SARS-CoV-2 infection at 2-4dpi, which was accompanied by clear evidence of apoptosis in the infected mOSNs. mOSN are the odorant receptor cells that are responsible for detection of odor and transduction of olfactory signal from nasal cavity to the glomeruli of olfactory bulbs [31], SARS-CoV-2 infection and damage of mOSN could directly contribute to the loss of smell in COVID-19 patients.

Olfactory neurons retain the unique capacity of regeneration from the stem and progenitor cells, the globose basal cells (GBC) and the horizontal basal cells (HBC). Current

clinical data suggested that olfactory dysfunction in COVID-19 patients are mostly transient [27] and thus the damages to olfactory neurons might be reversible. Our findings demonstrated that SARS-CoV-2 could infect the newly generated Tuj1-expressing iOSN. In addition, the cells at the basal layer of hamster OE were also infected, implying the regeneration capacity of OE could potentially be compromised by SARS-CoV-2 infection. Though our histology study of OE showed sign of epithelial cell proliferation and recovery of tissue structure at 7dpi and 14dpi, one of the limitations here is the lack of information on SARS-CoV-2 infection in olfactory neuronal stem cells. Further study is needed for a better understanding on the tissue regeneration process.

Each olfactory sensory neuron projects a dendrite into the nasal cavity on the apical side, and on the basal side extends its axon through the cribriform plate into the olfactory bulb of the brain, which in a sense can serve as a port for virus spread from the nasal cavity to the central never system (CNS). Instances of brain infection through olfactory nerves have been reported in influenza A viruses, adenoviruses, paramyxoviruses, herpesviruses, and vesicular stomatitis virus infections [32]. COVID-19 patients with neurological symptoms such as dizziness, headache, impaired consciousness [33, 34] and the detection of SARS-CoV-2 RNA in the cerebrospinal fluid (CSF) [35] suggested the possibility of central nervous system infection by SARS-CoV-2. In our previous study, the RNA load at 4dpi was low in homogenized hamster brain tissues. Furthermore, no NP antigen was detected from the olfactory bulb or other part of the brain at any time points examined. This suggested direct SARS-CoV-2 infection of the brain, if any, is a rare event. The occasionally detected TUNEL signal in the olfactory bulb might be due to inflammation-mediated apoptosis [36].

The COVID-19 pandemic is difficult to control by the conventional epidemiological control measures of testing symptomatic patients, isolation of the laboratory confirmed cases, and contact tracing and quarantine, because many have mild or no respiratory symptoms and would not have come forward and request RT-PCR testing [37]. Indeed a large proportion of COVID-19 cases were subclinical and only found in seroepidemiological studies [38, 39]. Even for those who subsequently developed respiratory symptoms, they are infectious before symptom onset. These epidemiological and clinical findings are consistent with our findings in ex vivo lung tissue explant culture which showed that SARS-CoV-2 completely suppresses the innate immune response by type 1 to 3 interferons and partially suppresses the proinflammatory chemokine/cytokine response [16, 40]. SARS-CoV-2 is primarily spread by respiratory droplets of more than 5-10μm in diameter which could be filtered by surgical mask as we previously shown in a hamster model [41]. Any unmasked individuals staying for a prolonged period within one to two meters from a COVID-19 patient could inhale the virus-laden respiratory droplets which would usually settle on the mucosa of their nasopharynx. The virus receptor ACE2 and the host protease TMPRSS2 for proteolytic activation of the viral Spike glycoprotein are abundantly found on the nasopharyngeal pseudo-columnar ciliated epithelial cells which are highly susceptible to SARS-CoV-2 as we and others have previously shown in the hamster model [17, 29]. However how this could lead to olfactory dysfunction is still debatable. Computed tomography of the paranasal sinuses of our six reported COVID-19 patients with olfactory dysfunction confirmed by butanol threshold test showed no radiological evidence of sinusitis [12]. Bilateral olfactory cleft obstructions were only found in two patients and partial obstruction in one patient. Moreover, their nasal biopsy showed minimal inflammatory changes with mild infiltrations of lymphocytes, plasma cells, and occasional

neutrophils in the epithelium and stroma which again did not support that inflammatory cytokine in causing olfactory neuronal dysfunction. A few of them had persistent and disabling anosmia of more than two months. Our previous study showed that the neuronal cell line U251 can modestly support the replication of SARS-CoV-2 but not SARS-CoV [16]. Consistent with the reported clinical manifestations of confusion, dizziness, meningoencephalitis, and Guillain-Barré syndrome, our findings supported the hypothesis that SARS-CoV-2 could infect mature and less mature progenitor OSN, and glial like supporting sustentacular cells as shown in our present study. Taken together these findings can explain the severe and prolonged anosmia in some COVID-19 patients despite the absence of infection in the olfactory bulb.

Our study is limited by the non-availability of human olfactory neuronal cell line or olfactory organoid for direct infection by SARS-CoV-2 which should provide more information on the kinetics of virus replication, and that of the response by cytokines and chemokines. In conclusion, our hamster study demonstrated SARS-CoV-2 productively infected olfactory neurons including mOSN and iOSN of hamsters and induced apoptosis. In addition, SARS-CoV-2 also infected sustentacular cells and submucosal glands that might adversely impact the viability and function of olfactory neurons. The direct virus-mediated OE damage and the virus-induced inflammatory response potentially explained the olfactory dysfunction in COVID-19 patients. Further studies on OSN regeneration following SARS-CoV-2 infection are warranted.

AUTHOR CONTRIBUTIONS

A.J.Z., H.C., J.F.-W.C., and K.-Y.Y. conception or design of the work. A.J.Z., A.C-Y.L., H.C., Z.F., C.L., F.L., Y.C., S.Y., V.K.-M.P., C.C.-S.C., K.L.-K.W., Y.S.C., J.-P.C., S.S., J.F.-W.C., and K.-Y.Y. acquisition, analysis, or interpretation of data. A.J.Z., H.C., J.F.-W.C., and K.-Y.Y. drafted manuscript.

Funding: This study was partly supported by the donations of the Shaw Foundation Hong Kong, Richard Yu and Carol Yu, May Tam Mak Mei Yin, Michael Seak-Kan Tong, Respiratory Viral Research Foundation Limited, Hui Ming, Hui Hoy and Chow Sin Lan Charity Fund Limited, Chan Yin Chuen Memorial Charitable Foundation, Marina Man-Wai Lee, the Hong Kong Hainan Commercial Association South China Microbiology Research Fund, the Jessie & George Ho Charitable Foundation, Perfect Shape Medical Limited, Kai Chong Tong, Foo Oi Foundation Limited, and Lo Ying Shek Chi Wai Foundation; and funding from the Health and Medical Research Fund (grant no. COVID190121), the Food and Health Bureau, The Government of the Hong Kong Special Administrative Region; the National Program on Key Research Project of China (grant no. 2020YFA0707500 and 2020YFA0707504); the Consultancy Service for Enhancing Laboratory Surveillance of Emerging Infectious Diseases and Research Capability on Antimicrobial Resistance for Department of Health of the Hong Kong Special Administrative Region Government; and the Theme-Based Research Scheme (T11/707/15) of the Research Grants Council, Hong Kong Special Administrative Region. The funding sources had no role in the study design, data collection, analysis, interpretation, or writing of the report.

DECLARATION OF INTERESTS

All author declares no competing interests

REFERENCES

1. Zhu N, Zhang D, Wang W, et al. A Novel Coronavirus from Patients with Pneumonia in China, 2019. N Engl J Med **2020**; 382(8): 727-33.
2. Chan JF, Yuan S, Kok KH, et al. A familial cluster of pneumonia associated with the 2019 novel coronavirus indicating person-to-person transmission: a study of a family cluster. Lancet **2020**; 395(10223): 514-23.
3. Chan JFW, K-H K, Zhu Z, et al. Genomic characterization of the 2019 novel human-pathogenic coronavirus isolated from a patient with atypical pneumonia after visiting Wuhan (vol 23, pg 2511, 2019). Emerg Microbes Infec **2020**; 9(1): 540-.
4. Cucinotta D, Vanelli M. WHO Declares COVID-19 a Pandemic. Acta Biomed **2020**; 91(1): 157-60.
5. World Health Organization. Coronavirus disease 2019 (COVID-19) Situation Report - 166. Available at: https://www.who.int/docs/default-source/coronaviruse/situation-reports/20200704-covid-19-sitrep-166.pdf?sfvrsn=6247972_2. Accessed 5/7/2020.
6. Guan WJ, Ni ZY, Hu Y, et al. Clinical Characteristics of Coronavirus Disease 2019 in China. N Engl J Med **2020**; 382(18): 1708-20.
7. Yan CH, Faraji F, Prajapati DP, Boone CE, DeConde AS. Association of chemosensory dysfunction and Covid-19 in patients presenting with influenza-like symptoms. Int Forum Allergy Rhinol **2020**.
8. Galougahi MK, Ghorbani J, Bakhshayeshkaram M, Naeini AS, Haseli S. Olfactory Bulb Magnetic Resonance Imaging in SARS-CoV-2-Induced Anosmia: The First Report. Acad Radiol **2020**.
9. Gane SB, Kelly C, Hopkins C. Isolated sudden onset anosmia in COVID-19 infection. A novel syndrome? Rhinology **2020**.
10. Giacomelli A, Pezzati L, Conti F, et al. Self-reported olfactory and taste disorders in SARS-CoV-2 patients: a cross-sectional study. Clin Infect Dis **2020**.
11. Lechien JR, Chiesa-Estomba CM, De Siati DR, et al. Olfactory and gustatory dysfunctions as a clinical presentation of mild-to-moderate forms of the coronavirus disease (COVID-19): a multicenter European study. Eur Arch Oto-Rhino-L **2020**.
12. Chung TW, Sridhar S, Zhang AJ, et al. Olfactory Dysfunction in Coronavirus Disease 2019 Patients: Observational Cohort Study and Systematic Review. Open Forum Infect Dis **2020**; 7(6): ofaa199.
13. Goncalves S, Goldstein BJ. Pathophysiology of Olfactory Disorders and Potential Treatment Strategies. Curr Otorhinolaryngol Rep **2016**; 4(2): 115-21.
14. Seiden AM. Postviral olfactory loss. Otolaryng Clin N Am **2004**; 37(6): 1159-+.
15. Suzuki M, Saito K, Min WP, et al. Identification of viruses in patients with postviral olfactory dysfunction. Laryngoscope **2007**; 117(2): 272-7.

16. Chu H, Chan JF-W, Yuen TT-T, et al. Comparative tropism, replication kinetics, and cell damage profiling of SARS-CoV-2 and SARS-CoV with implications for clinical manifestations, transmissibility, and laboratory studies of COVID-19: an observational study. The Lancet Microbe **2020**.
17. Chan JF, Zhang AJ, Yuan S, et al. Simulation of the clinical and pathological manifestations of Coronavirus Disease 2019 (COVID-19) in golden Syrian hamster model: implications for disease pathogenesis and transmissibility. Clin Infect Dis **2020**.
18. Chan JF, Yip CC, To KK, et al. Improved Molecular Diagnosis of COVID-19 by the Novel, Highly Sensitive and Specific COVID-19-RdRp/Hel Real-Time Reverse Transcription-PCR Assay Validated In Vitro and with Clinical Specimens. J Clin Microbiol **2020**; 58(5).
19. Lee AC, He JW, Ma MH. Olfactory Marker Protein Is Critical for Functional Maturation of Olfactory Sensory Neurons and Development of Mother Preference. J Neurosci **2011**; 31(8): 2974-82.
20. Chen M, Reed RR, Lane AP. Acute inflammation regulates neuroregeneration through the NF-kappaB pathway in olfactory epithelium. Proc Natl Acad Sci U S A **2017**; 114(30): 8089-94.
21. Salazar I, Quinteiro PS. The risk of extrapolation in neuroanatomy: the case of the mammalian vomeronasal system. Front Neuroanat **2009**; 3.
22. Geisert Jr E, Frankfurter A. The neuronal response to injury as visualized by immunostaining of class III β-tubulin in the rat. Neuroscience letters **1989**; 102(2-3): 137-41.
23. Holbrook EH, Wu E, Curry WT, Lin DT, Schwob JE. Immunohistochemical characterization of human olfactory tissue. Laryngoscope **2011**; 121(8): 1687-701.
24. Kupke A, Wenisch S, Failing K, Herder C. Intranasal Location and Immunohistochemical Characterization of the Equine Olfactory Epithelium. Front Neuroanat **2016**; 10.
25. Brann D, Tsukahara T, Weinreb C, Logan D, Datta S. Non-neural expression of SARS-CoV-2 entry genes in the olfactory epithelium suggests mechanisms underlying anosmia in COVID-19 patients. bioRxiv **2020**.
26. Bilinska K, Jakubowska P, Von Bartheld CS, Butowt R. Expression of the SARS-CoV-2 Entry Proteins, ACE2 and TMPRSS2, in Cells of the Olfactory Epithelium: Identification of Cell Types and Trends with Age. ACS Chem Neurosci **2020**; 11(11): 1555-62.
27. Ralli M, Di Stadio A, Greco A, de Vincentiis M, Polimeni A. Defining the burden of olfactory dysfunction in COVID-19 patients. Eur Rev Med Pharmacol Sci **2020**; 24(7): 3440-1.
28. Tian J, Pinto JM, Cui XL, et al. Sendai Virus Induces Persistent Olfactory Dysfunction in a Murine Model of PVOD via Effects on Apoptosis, Cell Proliferation, and Response to Odorants. Plos One **2016**; 11(7).
29. Sia SF, Yan LM, Chin AWH, et al. Pathogenesis and transmission of SARS-CoV-2 in golden hamsters. Nature **2020**.
30. Bryche B, St Albin A, Murri S, et al. Massive transient damage of the olfactory epithelium associated with infection of sustentacular cells by SARS-CoV-2 in golden Syrian hamsters. bioRxiv **2020**: 2020.06.16.151704.
31. Albeanu DF, Provost AC, Agarwal P, Soucy ER, Zak JD, Murthy VN. Olfactory marker protein (OMP) regulates formation and refinement of the olfactory glomerular map. Nat Commun **2018**; 9(1): 5073.
32. van Riel D, Verdijk R, Kuiken T. The olfactory nerve: a shortcut for influenza and other viral diseases into the central nervous system. J Pathol **2015**; 235(2): 277-87.
33. Mao L, Jin H, Wang M, et al. Neurologic Manifestations of Hospitalized Patients With Coronavirus Disease 2019 in Wuhan, China. JAMA Neurol **2020**.
34. De Felice FG, Tovar-Moll F, Moll J, Munoz DP, Ferreira ST. Severe Acute Respiratory Syndrome Coronavirus 2 (SARS-CoV-2) and the Central Nervous System. Trends Neurosci **2020**; 43(6): 355-7.
35. Moriguchi T, Harii N, Goto J, et al. A first case of meningitis/encephalitis associated with SARS-Coronavirus-2. Int J Infect Dis **2020**; 94: 55-8.

36. Aktas O, Ullrich O, Infante-Duarte C, Nitsch R, Zipp F. Neuronal damage in brain inflammation. Arch Neurol **2007**; 64(2): 185-9.
37. Hung IF, Cheng VC, Li X, et al. SARS-CoV-2 shedding and seroconversion among passengers quarantined after disembarking a cruise ship: a case series. The Lancet Infectious diseases **2020**.
38. To KK-W, Cheng VC-C, Cai J-P, et al. Seroprevalence of SARS-CoV-2 in Hong Kong and in residents evacuated from Hubei province, China: a multicohort study. The Lancet Microbe **2020**.
39. Xu X, Sun J, Nie S, et al. Seroprevalence of immunoglobulin M and G antibodies against SARS-CoV-2 in China. Nat Med **2020**.
40. Chu H, Chan JF, Wang Y, et al. Comparative replication and immune activation profiles of SARS-CoV-2 and SARS-CoV in human lungs: an ex vivo study with implications for the pathogenesis of COVID-19. Clin Infect Dis **2020**.
41. Chan JF, Yuan S, Zhang AJ, et al. Surgical mask partition reduces the risk of non-contact transmission in a golden Syrian hamster model for Coronavirus Disease 2019 (COVID-19). Clin Infect Dis **2020**.

FIGURE LEGENDS

Figure 1. Histological structure of hamster olfactory epithelium (OE) and SARS-CoV-2 infection.

(A) Illustration of sampling location in the hamster nasal cavity (left). Representative image of haematoxylin and eosin (H&E) stained mock infected hamster OE (right). (B) Left: Illustration of different cell types in hamster OE. Right: Magnified images of immunofluorescence and H&E stained mock infected hamster OE. Olfactory marker protein (OMP, red) in the cytoplasm of mOSN (arrowheads); Neuron-specific class III β-tubulin protein (Tuj1, red) in the cell body, dendrite and axon of iOSN (open arrowheads). DAPI, blue. (C) Viral load and $TCID_{50}$ titer in nasal turbinate tissues. 10^5 PFU of SARS-CoV-2 were inoculated to hamsters via intranasal route. At 2, 4 and 7 days after virus infection, nasal turbinate tissues were taken and homogenized for viral load determined by quantitative real time RT-PCR (left); infectious viral titer were determined by $TCID_{50}$ assay in VeroE6 cells (right). N=3 each group. Data represented mean ± SD. * $p < 0.05$, ** $p < 0.01$, ***$p < 0.001$ by one-way ANOVA. (D) Images of H&E stained SARS-CoV-2 infected hamster OE and immunofluorescence stained SARS-CoV-2 NP in formalin fixed nasal turbinate tissues sections at 12 hpi, 2, 4, and 7dpi. At 12hpi, H&E image showed intact epithelium with mild submucosal infiltration (black arrows). NP (green) expressing cells were scattered in the epithelium (arrowheads) and detached tissue debris (white arrow). At day 2 and 4dpi, H&E image showed OE desquamation and luminal cell debris (black arrows). NP (green) expressing cells evidently increased from scattered distribution in OE at 2dpi to diffuse distribution from apical surface to basal layer of OE at 4dpi (white arrowheads); luminal debris associated NP also shown (white arrows). At day 7, the images showed intact OE

structure with some degree of infiltration, large patch of tissue debris in the lumen (black arrows). NP was only showed in the luminal debris but not in the intact OE. Boxed areas were magnified.

Scale bars, 20µm (A and B), 200µm (D). OE, olfactory epithelium; LP, lamina propria; OSN, olfactory sensory neurons; mOSN, mature OSN; iOSN, immature OSN; BG, Bowman's gland; SC, sustentacular cells; BC, basal cells.

Figure 2. Expression of SARS-CoV-2 NP in different cell types in the OE of hamster at 4dpi.

(A) Immunofluorescence images showed lager amount of SARS-CoV-2 NP expression in respiratory epithelial cells of hamster nasal cavity at 4dpi (arrowheads). (B) Magnified immunofluorescence images indicated different morphology of NP expressing cells in hamster OE, which resemble olfactory sensory neuron (OSN), sustentacular cells (SC), horizontal basal cell (BC) and Bowman's glands (BG). (C) Images of double immunofluorescence stained SARS-CoV-2 NP (green) and olfactory neuron marker OMP (red) in hamster OE at 4dpi, merged image showing NP expression in the OMP expressing neuron layer. Magnified images in the bottom panel showed co-localization of NP with OMP expressing neurons (arrowheads). (D) Magnified immunofluorescence images indicated OMP expressing mOSN express NP (arrowheads). (E) Images of double immunofluorescence stained NP (green) and neuron marker Tuj1 (red) in hamster OE. Arrowheads in magnified images indicated co-localization of NP with Tuj1. Arrows indicated the infected sustentacular cells in the apical region of the OE.

DAPI, blue. Scale bars: 50µm (B), 10µm (C and E).

Figure 3. SARS-CoV-2 induced cytokine/chemokine responses and tissue damages in olfactory tissue of hamsters at 4dpi.

(A) Relative expression of IL-1β, IL-6, TNF-α, MIP1-α, RANTES, IP-10, IFN-α and IFN-γ, in homogenized nasal turbinated tissues determined by quantitative real time RT-PCR assay at 2, 4, and 7dpi. Mock infected hamsters were as controls. N=3 each group. Data represented mean ± SD. * $p < 0.05$, ** $p < 0.01$, *** $p < 0.001$ by one-way ANOVA. (B) H&E images at 4dpi showing destruction and massive infiltration of the OE (left, arrows); the image in the middle showed loss of whole apical layer of OE (arrowheads) and large amount of luminal secretion with cell debris (arrows). Image on the right showed the olfactory epithelium from mock infected hamster as control. (C) In the left panel, H&E image of the destructed olfactory tissue (upper) showing lots of TUNEL positive cells (green, lower). In the middle, double immunofluorescence staining of TUNEL (green) and OMP (red) showing detached mOSNs (arrows, upper), and also undetached mOSNs (arrows, lower) that were TUNEL positive. Images on the right showing the olfactory epithelium from mock infected hamster that are negative for TUNEL. Scale bar, 50μm.

Figure 4. Olfactory epithelial cell proliferation at 7 and 14dpi.

(A) OE tissues at 7dpi with relatively intact epithelium showed in H&E image, immunofluorescence stained cell proliferation marker Ki67 expression (red) was seen in the apical row and basal layer indicating proliferating cells (arrows). The boxed area was magnified. (B) OE tissues sampled at 14dpi with intact OE structure in H&E images; Ki67 expression was mainly detected in basal layer of the OE (arrows). The boxed area was magnified. Scale bar, 100μm. dpi, days post-infection; Neuron-specific class III β-tubulin protein.

Figure 1

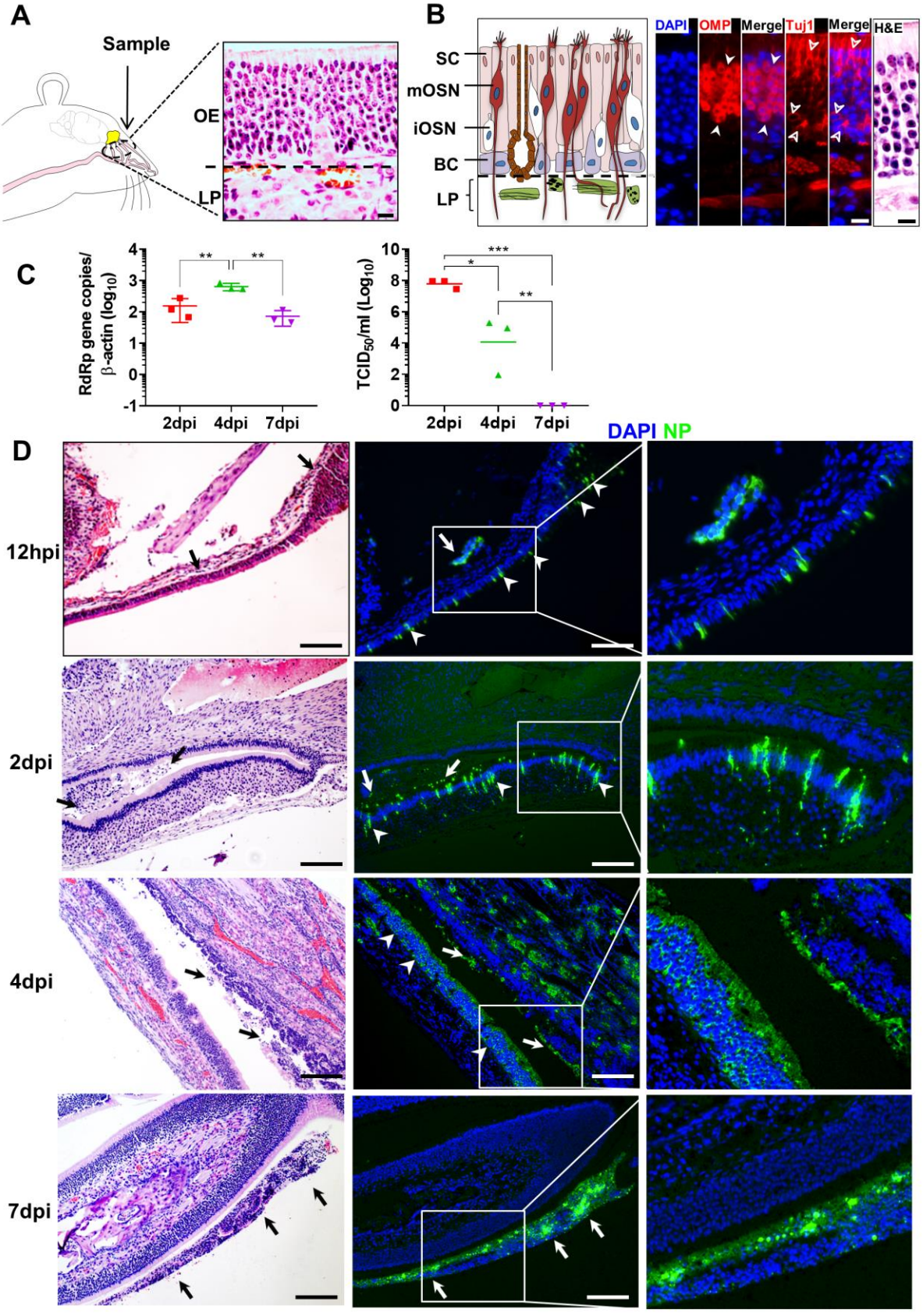
A
Sample
OE
LP
B
SC
mOSN
iOSN
BC
LP
DAPI
OMP
Merge
Tuj1
Merge
H&E
C
RdRp gene copies/ β-actin (log10)
2dpi
4dpi
7dpi
TCID50/ml (Log10)
2dpi
4dpi
7dpi
D
DAPI NP
12hpi
2dpi
4dpi
7dpi

Figure 2

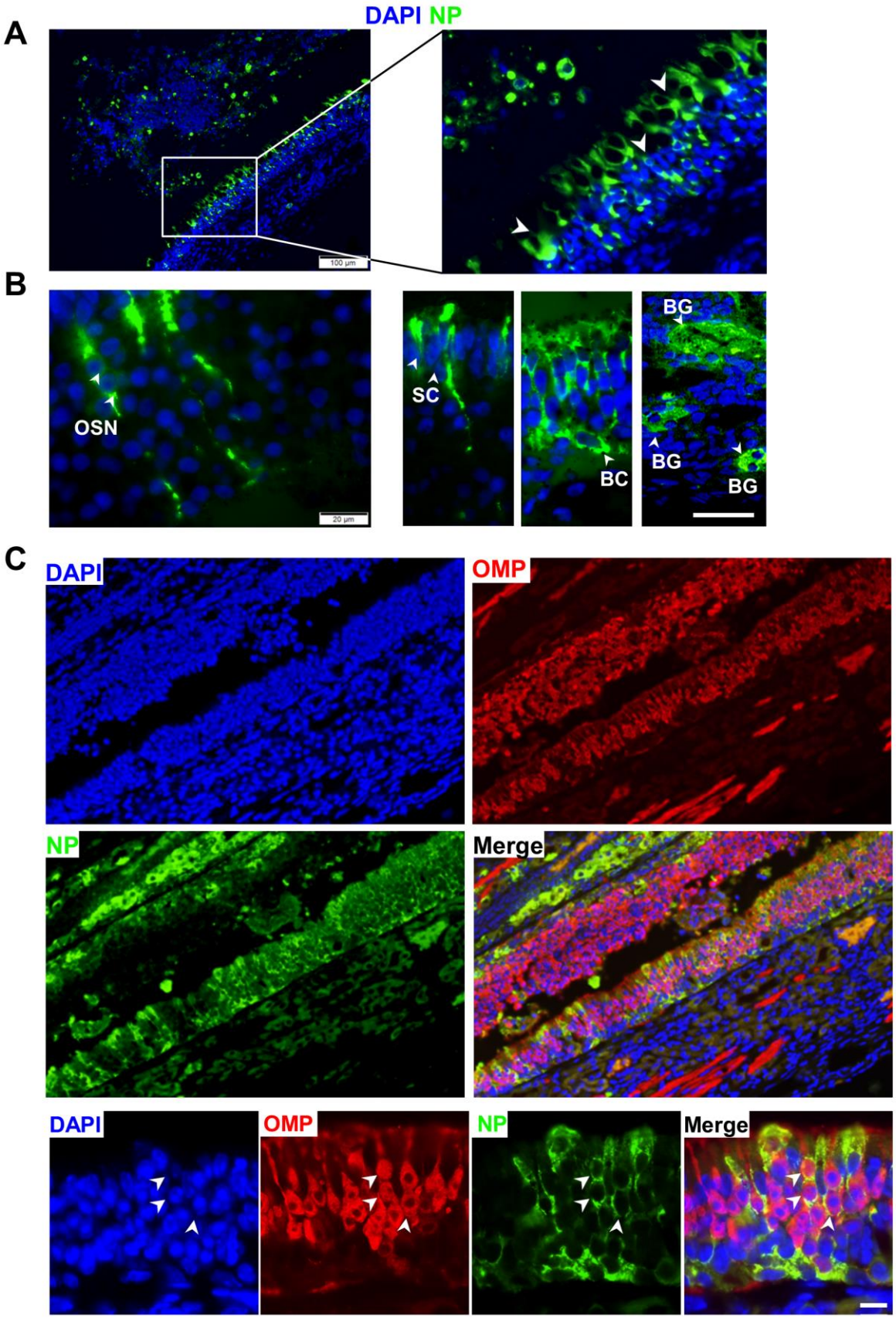
A
DAPI NP
100 μm
B
OSN
SC
BC
BG
BG
BG
20 μm
C
DAPI
OMP
NP
Merge
DAPI
OMP
NP
Merge

Figure 2

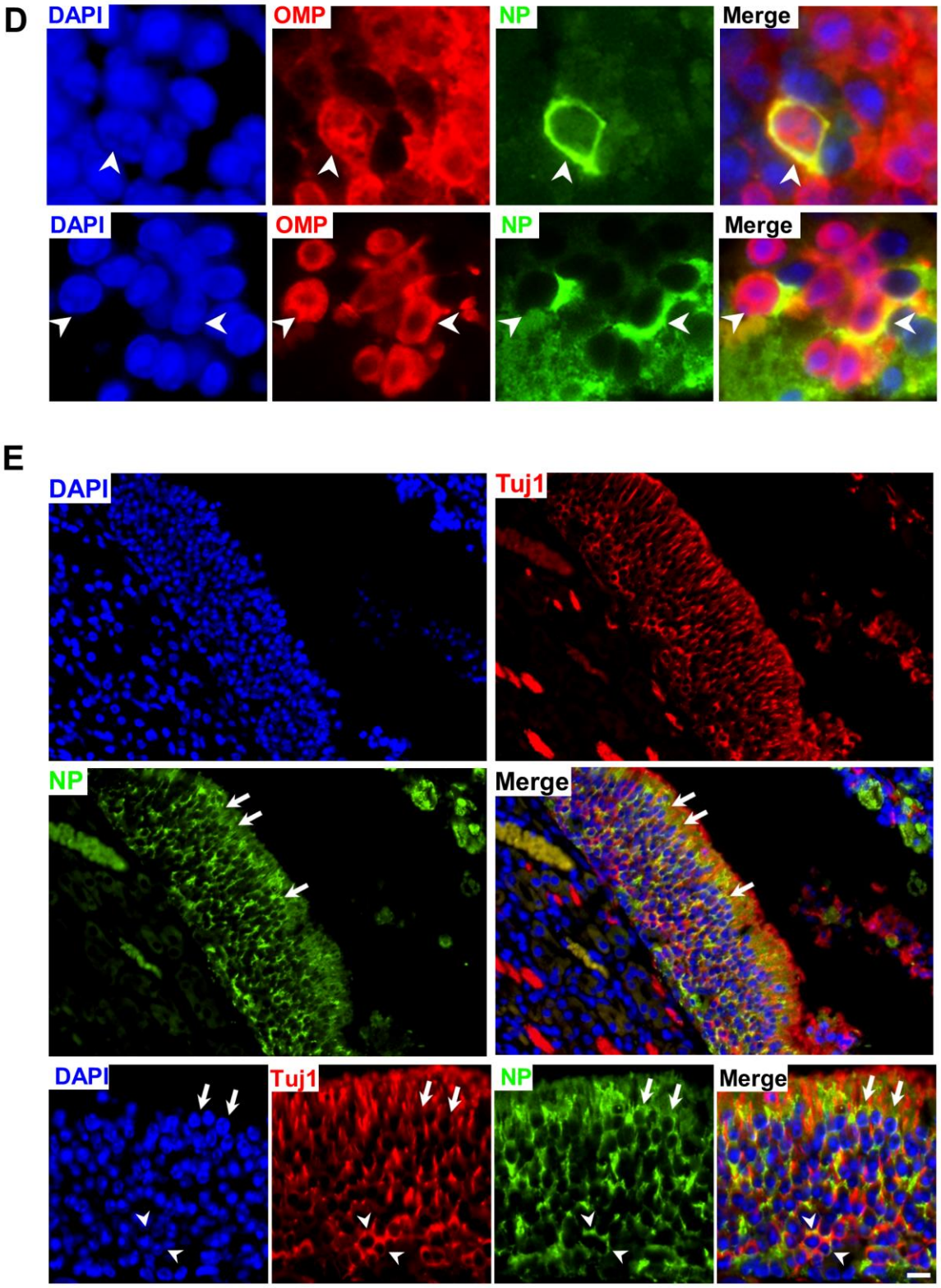
D
DAPI
OMP
NP
Merge
DAPI
OMP
NP
Merge
E
DAPI
Tuj1
NP
Merge
DAPI
Tuj1
NP
Merge

Figure 3

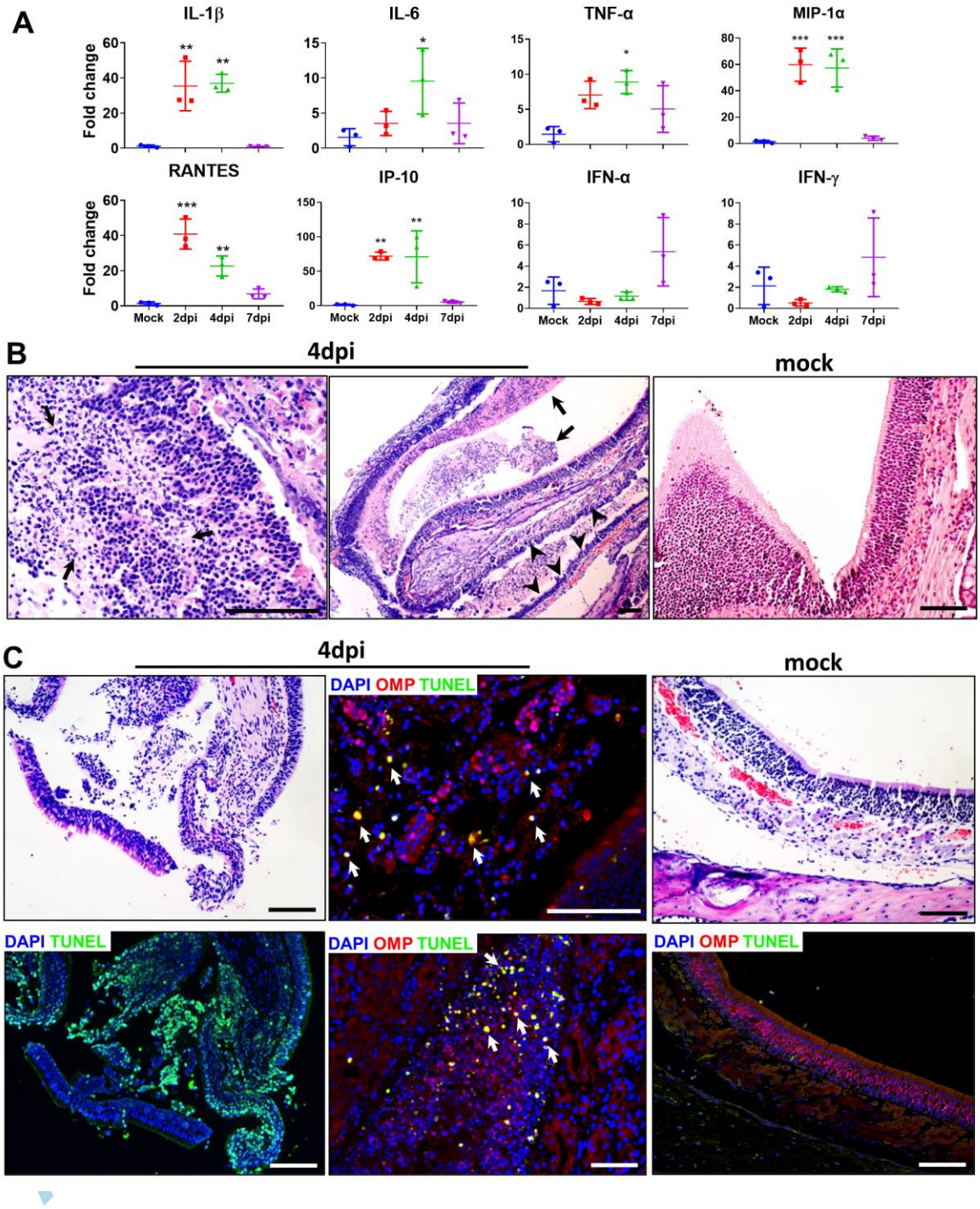
A
IL-1β
IL-6
TNF-α
MIP-1α
RANTES
IP-10
IFN-α
IFN-γ
Fold change
Mock
2dpi
4dpi
7dpi
B
4dpi
mock
C
4dpi
mock
DAPI OMP TUNEL
DAPI TUNEL
DAPI OMP TUNEL
DAPI OMP TUNEL

Figure 4